NANO LETTERS

2007
Vol. 7, No. 10
3241−3245

Diameter-Dependent Composition of Vapor–Liquid–Solid Grown $Si_{1-x}Ge_x$ Nanowires

Xi Zhang, Kok-Keong Lew,† Pramod Nimmatoori, Joan M. Redwing, and Elizabeth C. Dickey*

Department of Materials Science and Engineering, Materials Research Institute, The Pennsylvania State University, University Park, Pennsylvania 16802

Received May 15, 2007; Revised Manuscript Received August 6, 2007

ABSTRACT

Diameter-dependent compositions of $Si_{1-x}Ge_x$ nanowires grown by a vapor–liquid–solid mechanism using SiH_4 and GeH_4 precursors are studied by transmission electron microscopy and X-ray energy dispersive spectroscopy. For the growth conditions studied, the Ge concentration in $Si_{1-x}Ge_x$ nanowires shows a strong dependence on nanowire diameter, with the Ge concentration decreasing with decreasing nanowire diameter below ~50 nm. The size-dependent nature of Ge concentration in $Si_{1-x}Ge_x$ NWs is strongly suggestive of Gibbs–Thomson effects and highlights another important phenomenon in nanowire growth.

$Si_{1-x}Ge_x$ nanowires (NWs) have gained increasing significance because of the interest in semiconductor nanowire technologies as a potential pathway to the fabrication of sub-20 nm transistors.[1,2] To implement $Si_{1-x}Ge_x$ NW building blocks for nanoscale semiconductor devices, the NW chemical composition has to be carefully considered and precisely controlled because the chemical composition will ultimately determine the device performance.[3] There have been several previous studies investigating the Ge concentration in $Si_{1-x}Ge_x$ NWs.[4−7] For example, Duan et al.[4] have investigated $Si_{1-x}Ge_x$ NWs grown by laser-assisted catalytic growth (LCG) and found the Ge concentration in the $Si_{1-x}Ge_x$ NWs to be dependent on the location of nanowire growth in the chamber. By using this approach, it is not practical to systematically control composition during nanowire growth. Chemical vapor deposition (CVD) or molecular beam epitaxy (MBE) are alternative methods to grow $Si_{1-x}Ge_x$ NWs with maximum flexibility in composition control during the growth.[5,6] Recent work by Lew et al.[7] investigated the effect of growth temperature and gas-phase composition on the Ge concentration in $Si_{1-x}Ge_x$ NWs grown by VLS at low pressure using SiH_4 and GeH_4 precursors. It was found that growth temperature and gas-phase composition both influence Ge concentration in $Si_{1-x}Ge_x$ NWs, with higher temperatures (>375 °C) favoring the growth of Si-rich $Si_{1-x}Ge_x$ NWs and lower temperatures (<375 °C) favoring the growth of Ge-rich $Si_{1-x}Ge_x$ NWs. The entire compositional range of $Si_{1-x}Ge_x$ could be grown by varying the gas-phase composition and temperature. Size effects on $Si_{1-x}Ge_x$ nanowire composition have not, thus far, been addressed. In this letter, we study the influence of the nanowire diameter on the Ge concentration in $Si_{1-x}Ge_x$ NWs grown via Au catalyst CVD on Si (111) substrates or in nanoporous alumina membranes.

$Si_{1-x}Ge_x$ NWs in this study were grown by low-pressure CVD as described by Lew et al.[7] Si (111) substrates coated with ~0.2 μm thick Au thin films or anodized alumina membranes with 0.25 μm Au plugs electrodeposited in the pores near the top surface of the membrane were used as the substrates to grow the $Si_{1-x}Ge_x$ NWs. VLS growth was carried out at temperatures from 325 to 500 °C at a total reactor pressure of 13 Torr using a 10% mixture of SiH_4 in H_2 and 1% or 2% mixture of GeH_4 in H_2 as source gases. The total gas rate was held constant at 100 sccm. The GeH_4 concentrations were adjusted by varying the relative flow rates of the inlet gases, as summarized in Table 1.

Scanning electron microscopy (SEM, Philips XL20) was used for plan-view imaging of the $Si_{1-x}Ge_x$ NWs. Structural and chemical characterization of the NWs were carried out using a LaB_6 gun JEOL 2010 TEM operated at 200 kV and equipped with an X-ray energy dispersive spectrometer (EDS) for elemental analysis. In addition, some NWs were analyzed in a JEOL 2010F field-emission TEM/STEM (scanning TEM) also equipped with EDS. For TEM characterization, $Si_{1-x}Ge_x$ NWs were released from the substrate surface by sonication and suspended in semiconductor-grade isopropanol. The nanowire suspension was then dropped onto

* Corresponding author. E-mail: ecd10@psu.edu.
† Present address: Power Electronic Branch, Naval Research Laboratory, Washington, DC 20375.

10.1021/nl071132u CCC: $37.00
Published on Web 09/26/2007

Table 1. Growth conditions and fitted results of parameters d_{cSi}, d_{cGe}, and v_{0Si}/v_{0Ge} with eq 4

temperature (°C)	325 °C	425 °C	500 °C
$[GeH_4/((GeH_4 + SiH_4))]_{inlet\ gas}$	0.2	0.02	0.02
d_{cSi} (nm)	1.76 ± 0.27	1.92 ± 0.13	1.99 ± 0.21
d_{cGe} (nm)	6.9 ± 0.13	7.38 ± 0.15	8.48 ± 0.15
v_{0Si}/v_{0Ge}	0.17 ± 0.01	2.02 ± 0.01	5.28 ± 0.12

a lacey carbon-coated copper grid for TEM observation. Chemical compositions of $Si_{1-x}Ge_x$ NWs were quantified from the EDS data by the ζ method.[8] The ζ factor and k factors of the Si and Ge Kα X-ray emission lines used in the quantification were calibrated using a standard $Si_{1-x}Ge_x$ thin-film sample. The minimum detectable limit of Ge was about 0.8 atom %. It should be noted that the EDS signal originated from both the $Si_{1-x}Ge_x$ core and surface oxide, which makes the reported compositions representative of the as-grown wire composition before oxidation. Although not shown explicitly in this letter, we have shown via Monte Carlo simulations that the surface oxide introduces <2% change in the X-ray absorption even for the thinnest wires, so the EDS quantification scheme remains valid.

Figure 1a shows a SEM image of the synthesized NWs on Si (111). As previously reported,[9,10] $Si_{1-x}Ge_x$ NWs grow preferentially along the [111] direction. Figure 1b is a low-magnification bright-field TEM image of $Si_{1-x}Ge_x$ NWs. The alloy catalyst appears as a dark particle on the nanowire tip. The nanowire diameter is uniform along the entire length for every nanowire without tapering, which could result from thin-film deposition on the nanowire surfaces.[7] The crystalline nature of the NWs is characterized by high-resolution transmission electron microscopy (HRTEM) and selected area electron diffraction (SAD). The SAD pattern in Figure 1c confirms that nanowire growth occurs along the [111] direction. A uniform amorphous coating of ~3 nm thick is observed on the outer surface of the $Si_{1-x}Ge_x$ nanowires, as shown in Figure 1c, regardless of the core diameter. The chemical composition of the outer layer was found to be silicon oxide by EDS. The thickness uniformity of this surface oxide along the length of the wires indicated that it did not result from CVD deposition during growth but rather from post-growth surface oxidation. Figure 2 shows the diameter distributions of $Si_{1-x}Ge_x$ NWs grown at 325, 425, and 500 °C, respectively.

Before investigating the influence of diameter on the Ge concentration in $Si_{1-x}Ge_x$ NWs, the compositional homogeneity along the nanowire length was examined. Alloying homogeneity along the nanowire length was confirmed by collecting and quantifying a series of EDS spectra along the nanowire growth axis. One such EDS profile along the nanowire taken along the line in Figure 3a is presented in Figure 3b, with the counting statistic errors marked as error bars. The Si/Ge ratio is homogeneous along the nanowire.

Figure 4 shows the relationship between the Ge concentration and the diameter of the $Si_{1-x}Ge_x$ NWs. The experimentally obtained concentrations of Ge are plotted versus d at three growth temperatures of 325, 425, and 500 °C. The size-dependent nature of Ge concentration in $Si_{1-x}Ge_x$ NWs is

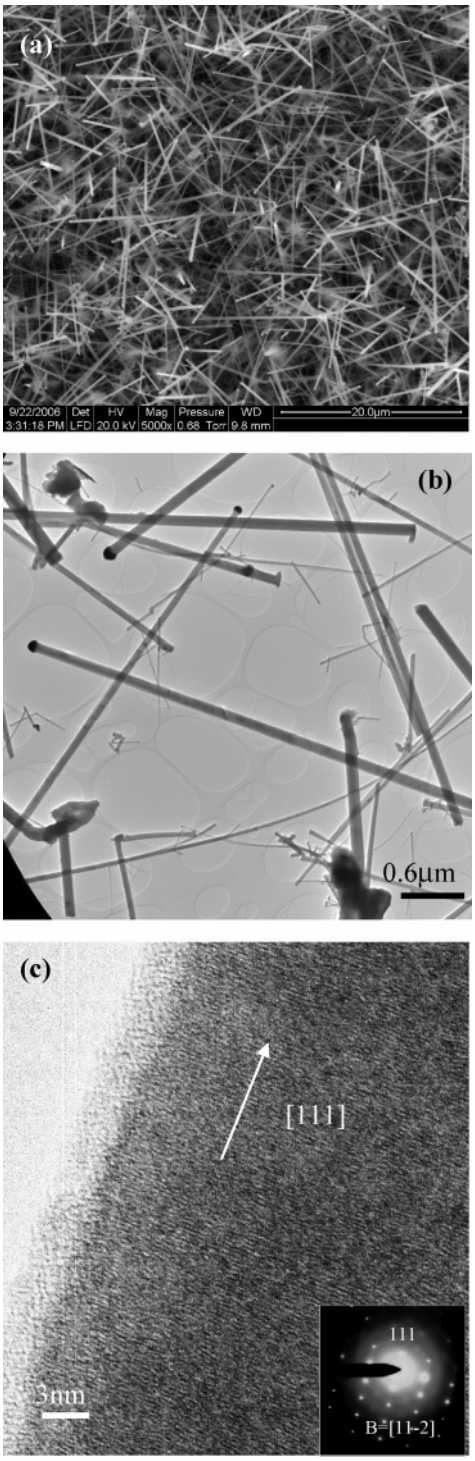

Figure 1. SEM and TEM images of $Si_{1-x}Ge_x$ nanowires grown at 425 °C with an inlet $GeH_4/(GeH_4+SiH_4)$ ratio of 0.02 (a) Plan-view SEM image of the $Si_{1-x}Ge_x$ nanowires on Si (111) substrates (b) Low-magnification bright-field TEM image of released $Si_{1-x}Ge_x$ nanowires (c) High-resolution TEM image of an individual $Si_{1-x}Ge_x$ nanowire with a [111] growth axis. The inset is the corresponding SADP. A uniform amorphous native oxide of ~3 nm thick is observed on the surface of the $Si_{1-x}Ge_x$ nanowire.

apparent in our experiments, with the Ge concentration increasing with nanowire diameter and converging to a constant composition at ~100 nm. The strong diameter dependence of the composition is suggestive of Gibbs-

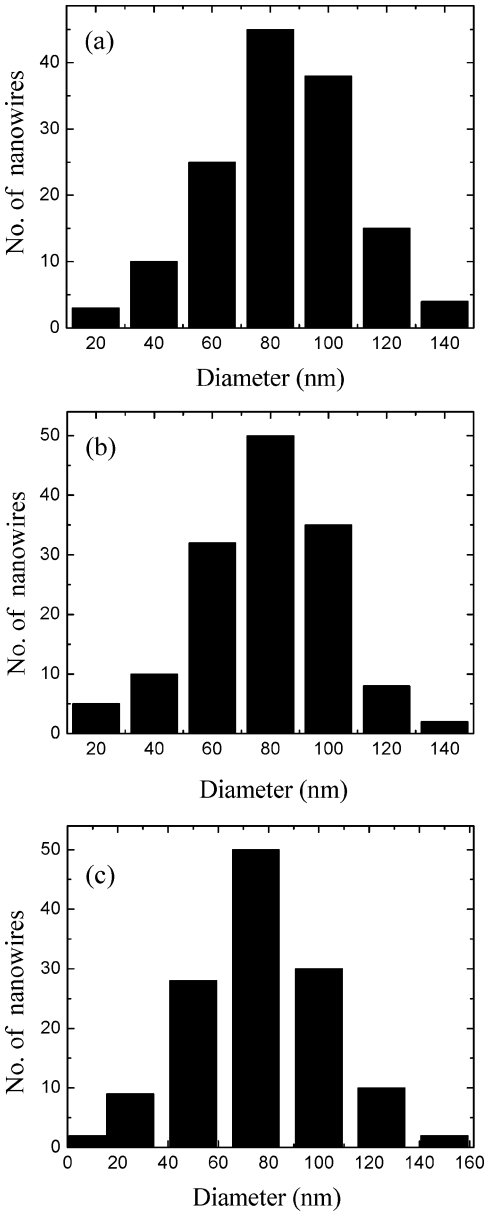

Figure 2. Diameter distributions of $Si_{1-x}Ge_x$ nanowires grown at different temperatures with an inlet $GeH_4/(GeH_4 + SiH_4)$ ratio of 0.023 (a) at 325 °C, (b) at 425 °C, and (c) at 500 °C.

Thompson, or surface tension, effects which have been observed to affect the growth rates of elemental Si nanowires.[9,11]

For elemental nanowires, by considering the kinetics of both the incorporation step at the catalyst surface and the crystallization step during the NW's growth, the relationship between the steady-state growth rate (v) and nanowire diameter (d) can be written as[9,11]

$$v = v_0 + \Gamma\frac{4\Omega^s\sigma^s}{d} \tag{1}$$

in which v_0 is the growth rate of NWs at $d \rightarrow \infty$, Ω^s is the molar volume in the solid phase, and σ^s is the surface tension of NWs. Γ is a factor independent of the NW diameter and is determined by the slopes of the incorporation velocities

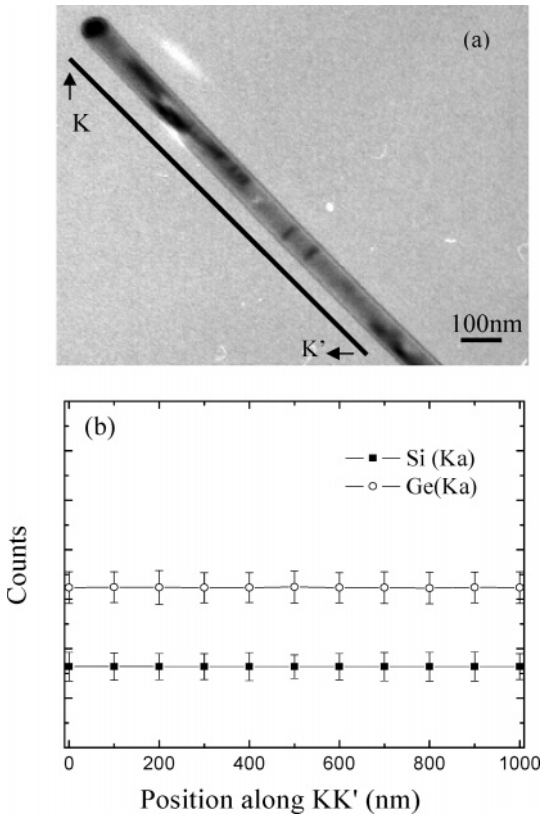

Figure 3. (a) TEM image of a $Si_{1-x}Ge_x$ nanowire grown at 425 °C, and (b) The EDS profiles taken along the line KK′ in (a), the EDS results indicates Si/Ge ratio is nearly homogeneous along the $Si_{1-x}Ge_x$ nanowires.

and crystallization velocities with respect to the catalyst droplet supersaturation.

When the growth rate $v = 0$, we obtain the inverse of critical diameter $1/d_c = -v_0/4\Omega^s\sigma^s\Gamma$, which is the kinetically allowed minimum NW diameter,[10] and then eq 1 can be rewritten as

$$v = v_0\left(1 - \frac{d_c}{d}\right) \tag{2}$$

In previous studies by our group, the Ge concentration (C_{Ge}) in $Si_{1-x}Ge_x$ NWs was empirically shown to be related to individual NW growth rate of Ge and Si over the growth temperature ranges of 325−425 °C:[7,12]

$$C_{Ge} = \frac{v_{Ge}}{v_{Si} + v_{Ge}} \tag{3}$$

where v_{Si} and v_{Ge} are the growth rate of Si and Ge, respectively. The previous study focused on nanowires around the most probable diameter where size effects were not strong. The linear relationship in eq 3 held best for Ge-rich growth regime with deviation from linearity in the lower Ge-content regime. Although this relationship is not completely satisfying in that it is empirically derived, it provides some framework to describe the size-dependent phenomenon in more detail.

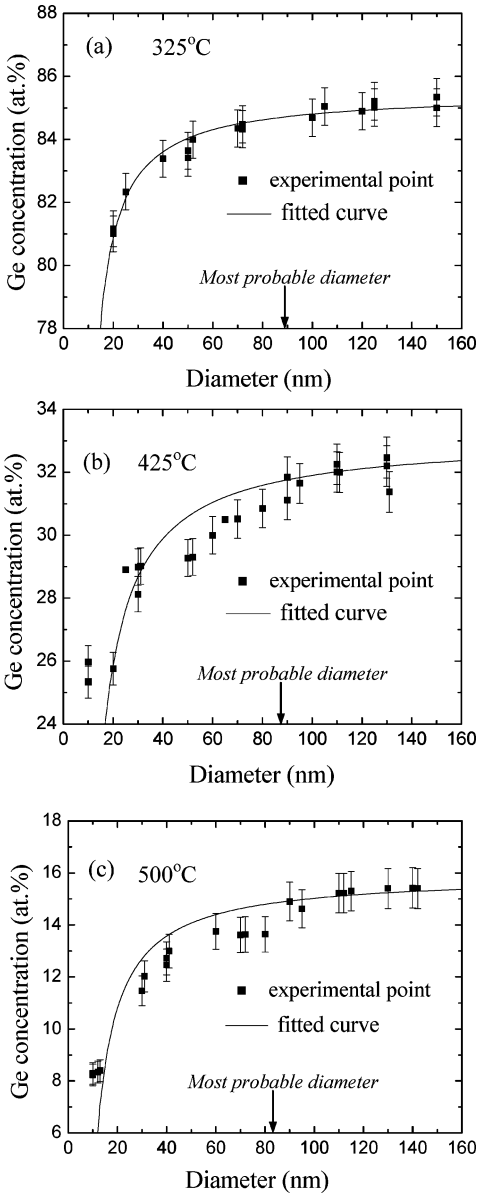

Figure 4. Relationship between the Ge concentration in $Si_{1-x}Ge_x$ nanowires and the diameter of $Si_{1-x}Ge_x$ nanowires grown at different temperatures (a) at 325 °C, (b) at 425 °C, and (c) at 500 °C.

Applying eq 2 to Si and Ge NW growth, respectively, and then substituting the growth rate of Si and Ge NWs into eq 3, the Ge concentration C_{Ge} can be related to the diameter (d) of NWs as follow

$$C_{Ge} = \frac{1}{1 + \left(\frac{v_{0Si}}{v_{0Ge}}\right)\left(\frac{d - d_{cSi}}{d - d_{cGe}}\right)} \quad (4)$$

Here d_{cSi} and d_{cGe} are the critical diameters of Si and Ge NWs; v_{0Si} and v_{0Ge} are the growth rates of Si and Ge NWs at $d \rightarrow \infty$. The Ge concentration in $Si_{1-x}Ge_x$ NWs can been predicted with eq 4, in which d_{cSi}, d_{cGe}, and v_{0Si}/v_{0Ge} are treated as the free fitting parameters in the model.

The solid curves in Figure 4a are obtained by fitting experimental points in Figure 4 with eq 4. The solid curves fit well with the experimental data corresponding to the 325 °C growth temperature where eq 3 is most valid.[7] The model fit is not as good for the lower Ge content wires grown at higher growth temperatures, indicating a more complex relationship governing the nanowire composition. Nonetheless, the overall trends in the size-dependent composition remain similar. The fitted results of parameters d_{cSi}, d_{cGe}, and v_{0Si}/v_{0Ge} are shown in Table 1.

In fact, in eq 4, when $d \gg d_{cSi}$ and d_{cGe}, $(d - d_{cSi})/(d - d_{cGe}) \approx 1$, the value of v_{0Si}/v_{0Ge} can be directly predicted from the experimental value of C_{Ge} at $d \gg d_{cSi}$ and d_{cGe} via eq 3. The values of v_{0Si}/v_{0Ge} are calculated as 0.17 at 325 °C, 2.03 at 425 °C, and 5.2 at 500 °C from experimental data in Figure 4. These values are very close to the fitted results of 0.17, 2.02, and 5.28 at the same growth temperatures, respectively. Moreover, the fitted results of d_{cSi} at three temperatures are 1.76, 1.92, and 1.99 nm agree well with the recently reported experimental minimum diameter of Si NWs of 1.7 nm[13] grown at temperatures between 365 and 495 °C via the VLS mechanism using gold as catalyst and SiH_4 as a vapor source and the theoretically predicted minimum size of stable Si crystallite with diamond-type structure around 1.8 nm grown by reduction of anhydrous ionic salt (e.g., SiX_4, where X = Cl, Br, or I) to Si using an anhydrous metal hydride in inverse micelles reaction vessels at room temperature.[14]

Although there are no experimental reports of d_{cGe}, our model predicts d_{cGe} is equal to 6.9, 7.38, and 8.48 nm at growth temperatures of 325, 425, and 500 °C, respectively. These values are reasonable because d_{cGe} can be theoretically predicted using the equation of $1/d_c = (\Delta\mu_0/kT)\,(kT/4\Omega\alpha_{vs})$[10] by comparing to d_{cSi}. Because

$$\frac{d_{cGe}}{d_{cSi}} = \frac{\Delta\mu_{0Si}\alpha_{vsGe}\Omega_{Ge}}{\Delta\mu_{0Ge}\alpha_{vsSi}\Omega_{Si}} \quad (5)$$

in which $\Delta\mu_0$ is the effective difference of the chemical potentials at the planar interface, α_{vs} is the specific surface free energy of the NWs, and Ω is the atomic volume. Parameters required for evaluation of eq 5 are as following: for VLS growth Si NWs, $\Delta\mu_{0Si} = 104.8$ kJ/mol[15,16] and $\alpha_{vsSi} = 1.14$ J/m^2;[17] for Ge NWs, $\Delta\mu_{0Ge} = 75.6$ kJ/mol[15,16] and $\alpha_{vsGe} = 0.88$ J/m^2.[17] The atomic volume ratio of Si and Ge is $\Omega_{Ge}/\Omega_{Si} \approx 2.2$.[18] Substituting these data into eq 5, we obtain $d_{cGe}/d_{cSi} \approx 2.4$. That indicates when $d_{cSi} \sim 2$ nm, $d_{cGe} \sim 5$ nm. Our fitted results of d_{cGe} approximately equal to this theoretically estimated d_{cGe}.

Furthermore we can see from the equation of $1/d_c = -v_0/4\Omega^s\sigma^s\Gamma$, wherein $v_0/\Omega^s\sigma^s > 0$, the sign of Γ only depends on the sign of d_c. Because the fitted d_{cSi} and d_{cGe} are both positive, $\Gamma$is negative, indicating the growth rate decreases with decreasing NW diameter for both Si and Ge in our growth conditions.[11]

In summary, we have prepared $Si_{1-x}Ge_x$ NWs using a CVD VLS method. By using quantitative EDS, the Ge concentration in $Si_{1-x}Ge_x$ NWs was investigated as a function of wire diameter. The Ge concentration in $Si_{1-x}Ge_x$ NWs was found to be strongly dependent on the NW diameter

below ∼50 nm. An empirical model was established to predict the composition of $Si_{1-x}Ge_x$ NWs by using size-dependent individual NWs growth rates of Ge and Si and incorporating size effects on the supersaturation of Si and Ge. The model fitted well with our experimental data for the 325 °C growth temperature, where the nanowire composition correlated well with the individual component growth rates. However, our approach was based on an empirical relationship for the alloy wire growth rates, and a more fundamental understanding of size effects in a three-component VLS system is needed.

Acknowledgment. This work was supported by the National Science Foundation NIRT program through grant number ECS 06-09282 and The Pennsylvania State University MRSEC for Nanoscale Science (DMR-0213623). TEM work was performed in the electron microscopy facility of the Materials Characterization Laboratory as part of The Pennsylvania State University's node of the NSF's National Nanotechnology Infrastructure Network (grant no. 0335765).

References

(1) Meyer, D. J.; Webb, D. A.; Ward, M. G.; Sellar, J. D.; Zeng, P. Y.; Robinson, J. *Mater. Sci. Semicond. Process.* **2001**, *4*, 529−533.
(2) Paul, D. J. *Thin Solid Films.* **1998**, *321*, 172−180.
(3) McCarthy, J.; Perova, T. S.; Moore, R. A.; Bhattacharya, S.; Gamble, H. S.; Armstrong, B. M. In Proceedings of the 1st International ICEEE conference on Electrical and Electronics Engineering, June 24−27, 2004; pp 226−230.
(4) Duan, X.; Lieber, M. C. *Adv. Mater.* **2000**, *12*, 298−302.
(5) Lew, K.-K.; Pan, L.; Dickey, E. C.; Redwing, J. M. *Adv. Mater.* **2003**, *15*, 2073−2076.
(6) Zakharov, N. D.; Werner, P.; Gerth, G.; Schubert, L.; Sokolov, L.; Gosele, U. *J. Cryst. Growth* **2006**, *290*, 6−10.
(7) Lew, K.-K.; Pan, L.; Dickey, E. C.; Redwing, J. M. *J. Mater. Res.* **2006**, *21*, 2876−2881.
(8) Watanabe, M.; Horita, Z.; Nemoto, M. *Ultramicroscopy* **1996**, *65*, 187−198.
(9) Wu, Y.; Fan, R.; Yang, P. *Nano Lett.* **2002**, *2*, 83−86.
(10) Givargizov, E. I. *J. Cryst. Growth* **1975**, *31*, 20−30.
(11) Schmidt, V.; Senz, S.; Gosele, U. *Phys. Rev. B* **2007**, *75*, 045335-1−045335-6.
(12) Redwing, J. M.; Dilts, S. M.; Lew, K. -K.; Cranmer, A. E.; Mohney, S. E. *Proc. SPIE* **2005**, *6003*, 60030S-1−60030S-7.
(13) Kikkawa, J.; Ohno, Y.; Takeda, S. *Appl. Phys. Lett.* **2005**, *86*, 123109−123111.
(14) Wilcoxon, J. P.; Samara, G. A. *Appl. Phys. Lett.* **1999**, *74*, 3164−3166.
(15) Kerr, J. A. *CRC Handbook of Chemistry and Physics 1999−2000: A Ready-Reference Book of Chemical and Physical Data*, 81st ed.; CRC Press: Boca Raton, FL, 2000.
(16) Cottrell, T. L. *Strengths of Chemical Bonds*, 2nd ed.; Butterworths: London, 1958; Darwent, B. D. *National Standard Reference Data Series No. 31*; National Bureau of Standards: Washington, DC, 1970; Benson, S. W. *J. Chem. Ed.* **1965**, *42*, 502−518.
(17) Jiang, Q.; Lu, H.; Zhao, M. *J. Phys.: Condens. Matter* **2004**, *16*, 521−530.
(18) Zeng, X.; Stroud, D. *J. Phys.: Condens. Matter* **1989**, *1*, 1779−1783.

NL071132U